

Toward Automated Calibration of Data Center Digital Twins: A Neural Surrogate Approach

Ruihang Wang¹, Yuanlong Li¹, Linsen Dong¹, Xin Zhou¹, Yonggang Wen¹, Rui Tan¹,
Li Chen², Guan Wang², Feng Zeng²

¹Nanyang Technological University, ²Alibaba Inc.

{ruihang001, liyuanl, lsdong, zhouxin, ygwen, tanrui}@ntu.edu.sg, {yuchi.cl, zibo.wg, zengfeng.zf}@alibaba-inc.com

Abstract—Evolving the computational fluid dynamics (CFD) model to high fidelity digital twin is desirable for industrial data center management. However, existing CFD model calibration approaches to improve the model accuracy require either excessive manual tuning or intensive computation, rendering them non-scalable with system size and complexity. This paper presents a surrogate-based approach to automate the calibration of CFD models built for industrial data centers. Specifically, a knowledge-based graph neural net (GNN) is trained to approximate a CFD model as a surrogate model that captures the key thermal variables and their causal relationships in a given data hall. By integrating prior knowledge as constraints, the GNN has reduced demand on the amount of training data. After rounds of the training processes, the neural surrogate can recommend the optimal configurations for the CFD model parameters that are hard to obtain, such that the temperatures predicted by the CFD are most consistent with the actual measurements. Experiments of applying the proposed approach to calibrate two CFD models built for two production data halls hosting thousands of servers achieve temperature prediction errors of 0.81°C and 0.75°C with about 30 hours of computation on a quad-core virtual machine in the cloud.

Index Terms—Data center, CFD modeling, Digital twin, Surrogate-based calibration, Graph neural net

I. INTRODUCTION

The scales of modern data centers have been continuously growing to meet the increasing cloud computing demands. According to a white paper from Cisco, the number of hyperscale data centers will double from 338 at the end of 2016 to 628 by 2021 [1]. The data centers' increases in size and complexity bring substantial challenges to efficient and effective management of their supporting infrastructures that aims to avoid operational risks and reduce energy costs.

The use of computerized data center management tools will help improve the competitiveness of a data center operator. Currently, data center infrastructure management (DCIM) system is a common tool to visualize and monitor the infrastructure status based on the measurements collected from many deployed hardware and software sensors [2]. DCIM provides the operator with useful and important information for proper response in case of abnormalities and failures. However, with the increases in system scale and complexity, it is desirable and imperative to extend DCIM to have accurate prediction capabilities. With such capabilities, the operator can perform

various what-if analysis, such as whether the increase of certain temperature setpoints can improve the energy efficiency without causing server overheating.

In this paper, we consider *digital twin* for the desired capability extension. Digital twin is a collection of integrated multi-physics, multi-scale, and probabilistic modeling and simulation techniques for as-built systems [3]. It aims to pursue high modeling accuracy for systems with ever-growing complexity based on data from various sources, including sensors, prior models, and domain knowledge. The concept was early applied in the aerospace industry for damage evaluation, cost reduction, and confidence assessment [4]–[6]. Recently, it has also attracted growing interest in other domains, such as smart manufacturing [7], cloud-based cyber-physical systems [8], and smart city creation [9]. To build digital twins for data centers, various elementary techniques from multiple disciplines have existed to model the cyber-physical processes from the building infrastructure level to the IT equipment chip level. In particular, the computational fluid dynamics (CFD) modeling is a primary technique to characterize the thermodynamics in data centers [10]. It has been widely adopted to explore the optimal operation policy for energy cost reduction and risk management in the offline analysis [11]. In this paper, we focus on constructing thermodynamic digital twins based on CFD modeling.

To achieve high CFD modeling accuracy, it is important to instrument the model with sufficiently complete configuration of the physical infrastructure. A model with incomplete configuration may diverge from the ground truth. For example, as reported in [12], [13], a raw CFD model can yield temperature prediction errors up to 5°C. Unfortunately, obtaining the complete system configuration often faces substantial challenges due primarily to 1) the large number of parameters in the configuration and 2) the extremely labor-intensive and error-prone manual calibration process for these parameters. For instance, each server in a data center may have its own characteristics of the passing-through air flow rate due to its internal fan control logic. However, such information is generally not available in the server hardware's specification and can only be empirically estimated or collected via *in situ* measurement. Therefore, for CFD modeling to evolve into its digital twin version, automated calibration of the difficult-to-obtain system configuration parameters will be

necessary. A number of heuristic algorithms (e.g., Bayesian optimization, genetic algorithms, simulated annealing, etc.) have been applied for such purpose [14], [15]. However, these algorithms require many search iterations to find good values for the system configuration parameters. In each iteration, a CFD simulation (i.e., model forwarding) is performed with the candidate parametric configuration. When the CFD is built for a complex data hall (hosting many servers), the iterative search process often incurs unacceptable computation time.

To advance automated CFD calibration beyond heuristic configuration search, we propose a surrogate-based approach for data centers with increasing scales and complexities. The proposed approach avoids direct forwarding of the CFD model with the help of a trainable neural net. Fig. 1 illustrates the workflow of the surrogate-based approach, in which the surrogate model iteratively updates the system configuration to minimize the CFD model’s prediction errors by two consecutive steps. First, the “coarse” surrogate is trained to align with the “fine” CFD model in the current system state locality by updating its internal weights. Second, the trained surrogate is re-optimized to update the system configuration, which is also a part of the neural net, to maximize the consistency between the surrogate’s predictions and the sensor measurements. Our approach aims to find the optimal configuration while requires the fewest CFD model forwarding processes. To achieve such objectives, we need to address the following two challenges. First, it is challenging to design the surrogate model to capture the complex thermodynamic laws encompassed in the CFD model. The vanilla approach of designing a neural net to approximate the CFD model as a black-box system may not yield satisfactory accuracy. Second, the training data for the surrogate model is limited since generating such data using the CFD model is computationally expensive and time-consuming.

To address the above challenges, we adopt the graph neural net (GNN) to build the surrogate model. The architecture of the GNN is designed to capture the prior knowledge of the thermal relations among a number of key variables in the physical infrastructure. The integration of the prior knowledge about the physical infrastructure improves the capability of the neural net in approximating the CFD model and reduces the demand on the amount of training data. We implement the surrogate-based approach and apply it to calibrate two CFD models of two production data halls sized hundreds of square meters that host thousands of servers, respectively. The CFD models calibrated using our GNN-based surrogate approach achieve mean absolute errors (MAEs) of 0.81°C and 0.75°C in predicting the temperatures at tens of positions in each hall, respectively. The calibration process takes about 30 hours on a quad-core virtual machine in the cloud. In contrast, the heuristic configuration search and the vanilla neural net-based surrogate approach achieve MAEs of around 4°C with the same computation time for calibration as our GNN-based surrogate. Such low accuracies are unsatisfactory for claiming digital twins. We also invite a domain expert to manually calibrate the two CFD models. The resulted MAEs are 1.32°C and 1.1°C, which are 0.51°C and 0.35°C higher than those

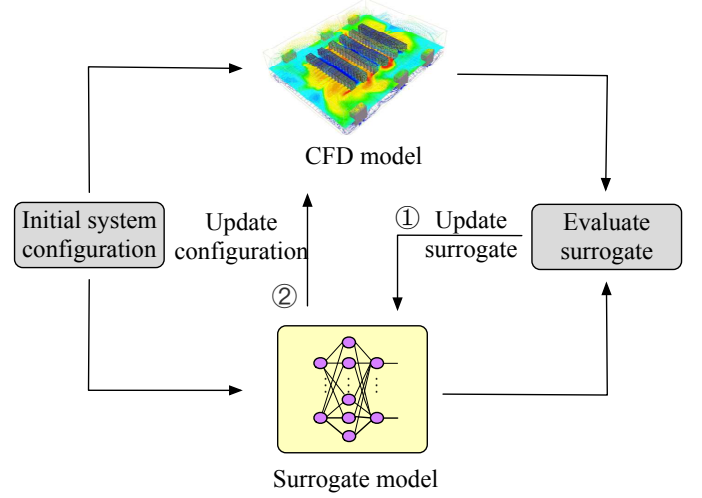


Fig. 1. Surrogate-based optimization for CFD model. First, the surrogate model is trained to approximate the CFD model. Second, the surrogate model updates the system configuration based on real sensor measurements. The two steps are iteratively executed to calibrate the system configuration.

achieved by our approach. Such an improvement is significant in CFD modeling due to the sharply increased difficulty in improving accuracy when the errors are already low (i.e., at around 1°C). The evaluation shows the effectiveness of our GNN-based surrogate approach in calibrating CFD models towards their digital twin versions.

The rest of the paper is structured as follows. §II reviews related work. §III formulates the automated calibration problem and presents the overview of our approach. §IV presents the design of the proposed knowledge-based neural surrogate. §V presents the evaluation of the proposed method for two production data halls. §VI concludes this paper.

II. RELATED WORK

In this section, we review the relevant research in data center modeling and surrogate-based optimization for complex models.

A. Data Center Modeling

A variety of modeling techniques have been proposed for thermal management and predictive maintenance in data centers. The modeling methods can be broadly categorized into law-based models, data-driven models, and hybrid models.

The CFD models are representative law-based models, as they capture the thermodynamic laws followed by the physical processes [10], [11], [13]. Their accuracy depends on the completeness of the system configuration provided. Moreover, the CFD models are computationally expensive due to their internal recursive execution. As the data centers become more complex, the CFD computation times may increase from hours to days, making the model calibration difficult. As reported in [12], [13], an uncalibrated CFD model can yield temperature prediction errors ranging from 2°C to 5°C, which are unsatisfactory for industry use. An alternative is to use black-box data-driven models to learn a thermal map in the data

center. For example, J. Moore et al. proposed Weatherman to predict the steady-state temperature distribution of a physical data center using artificial neural nets with error within 1°C in 92% of predictions [16]. D. Yi et al. designed a tandem long short-term memory (LSTM) networks to predict system state in [17]. The LSTM is trained offline to achieve a temperature prediction error of 1.24°C . Although these data-driven models avoid the requirement of complete system configuration and the computational challenges of using thermodynamics to solve the system state, they often perform poorly in the cases that are not covered by the training data. For instance, these models cannot well capture cooling system failures, because training data for such failure scenarios is generally lacking. To overcome these limitations, several hybrid methods of combining CFD models and data-driven models have been proposed. For instance, the ThermoCast system proposed by L. Li et al. integrates physical laws and sensor data to forecast temperature distribution [18]. J. Chen et al. used the data generated by a CFD model for rare scenarios to complement the actual sensor measurements to form the training dataset for a linear regression model for temperature distribution prediction [19]. To ensure fidelity, the CFD model used in [19] is manually calibrated by a human expert. As such, the approach is only evaluated on a small-size testbed.

B. Surrogate-Based Optimization

Parametric optimization is a fundamental task in computational model. It applies various strategies to search the optimal model configuration in terms of a defined objective function [20]. However, this approach, either gradient-based or derivative-free, often scales poorly with the size of the parameter space and the complexity of the model. Note that the parameter space size affects the number of search iterations; the model complexity affects the computation time of each search iteration. Surrogate-based optimization (SBO) is an alternative to avoid the direct optimization of such compute-intensive and undifferentiable models. It was first introduced by J. W. Bandler in linear space mapping between a coarse model and a fine model [21]. To date, several SBO approaches have been studied in lieu of direct optimization in electromagnetic simulators [22], hydrological models [23], and aerodynamic shape design [24]. Through proper design of the experiments, a number of training data generated from a high-fidelity model is used to build a lightweight surrogate. The design of the surrogate is application-specific. For example, low-fidelity law-based surrogates are usually built for full-fledged models in microwave engineering [25]. *Neural surrogates* designed based on artificial neural nets are used for high-dimensional and nonlinear models [12]. Surrogates designed based on vanilla neural nets often require excessive training data to achieve satisfactory performance.

In this paper, we focus on developing a surrogate-based calibration approach for complex data center CFD models. We aim to design a neural surrogate that provides satisfactory approximation accuracy while requires a small amount of training data generated from the CFD model. To the best of

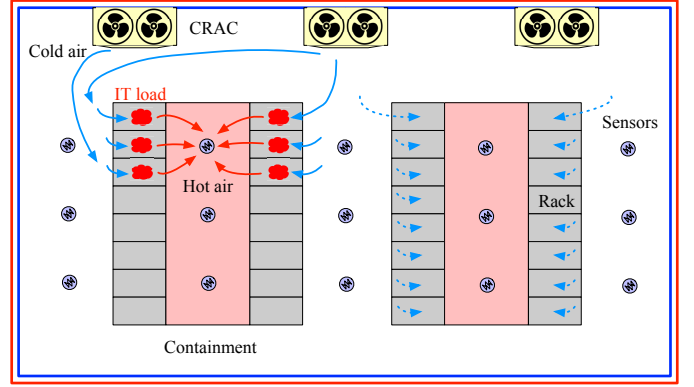


Fig. 2. The layout sketch of a typical data hall. Sensors are installed at the cold and hot aisles for cooling evaluation.

our knowledge, this paper presents the first work designing a knowledge-based neural surrogate that can calibrate the CFD models for industry-grade data centers.

III. PROBLEM FORMULATION AND APPROACH OVERVIEW

In this section, we first introduce the background of our work. Then, we formulate the problem and present the overview of our approach.

A. Background

CFD model can estimate the temperature and air velocity distributions in a given space by solving a simplified form of the Navier-Stokes equations [26]. For air-cooled data centers, CFD has been widely used as a predictive model for thermal and air flow analysis to avoid operational risks. To pursue higher efficiency of the cooling systems while not compromise the thermal safety of the computing and network equipment, it is desirable to improve the accuracy of the CFD model towards the paradigm of digital twin.

The layout of a data hall is typically sketched as Fig. 2, where *racks* hosting *servers* are assigned into multiple *rows* that separate *aisles*. These aisles alternate between cold and hot aisles. The *computer room air conditioning* units (CRACs) supply cold air to the servers through the cold aisles and draw hot air from the hot aisles. To avoid air recirculation, the containments are often implemented for the hot aisles. To evaluate the thermal condition in a data hall, the inlet and outlet temperatures of servers are often used as the key thermal variables. Therefore, temperature sensors are often deployed in the cold and hot aisles to monitor such thermal variables. The inlet temperatures are often required to be in the range of 15°C to 27°C [27]. The outlet temperatures characterize the heat generated by the servers. Although the CFD model can predict the temperature at any location, we focus on the locations that are deployed with temperature sensors and thus have ground truth temperature measurements for accuracy evaluation.

The servers in general have different characteristics in passing the cooling air through them. The characteristic highly depends on the server form factor and the control logics of the server's internal fans. Owing to the distinct characteristics, the

servers will have different passing-through air flow rates in cubic feet per minute watt (CFM/W), where the cubic feet is for air volume, the minute is for time, and the watt is for the server power. The collection of the server air flow rates is part of the system configuration that greatly affects the thermodynamics of the data hall. Therefore, to achieve high CFD accuracy, the server air flow rates should be provided to the CFD model. Unfortunately, they are often unknown and hard to obtain. The manual *in situ* measurement using an air volume flow rate meter for each server is extremely labor intensive, especially for a large-scale data hall that hosts many models of servers. As a result, the server air flow rates are often empirically estimated by human expert and configured into the CFD model. For a CFD model with many (e.g., thousands) of servers, the rough settings of the server air flow rates could significantly downgrade the temperature prediction capability of the CFD model. The low accuracy will impede the use of CFD model for the desired fine-grained operational adjustment to pursue energy efficiency without causing thermal risk.

In this paper, we focus on devising an automated approach to calibrate the server air flow rates configuration for data center CFD models. The approach can also be extended to include other parameters (e.g., by-pass air flow rates and recirculated air flow rates) into calibration. The calibration is based on a steady system state at a time instant. The system state consists of the following measurements: the supply air temperatures and fan speeds of CRAC units, server powers and the temperatures measured in the hot and cold aisles. With the calibrated server air flow rates, the CFD model is expected to yield more accurate temperature distribution prediction. Thus, the prediction accuracy of the calibrated CFD model at future time instants can be used as the main metric for evaluating the effectiveness of the calibration.

B. Problem Formulation

To formulate the calibration problem, we first define the relevant parameters in a data hall. We consider a data hall hosting l CRACs, m servers, and n temperature sensors deployed in the cold and hot aisles.

Definition 1 (Input): The input data for solving a CFD model is a vector consisting of all modeling parameters. Formally, the input $\mathbf{x} = [\mathbf{T}_c, \mathbf{V}, \mathbf{P}, \boldsymbol{\alpha}]$, where $\mathbf{T}_c = [T_{c1}, T_{c2}, \dots, T_{cl}]$, $\mathbf{V} = [V_1, V_2, \dots, V_l]$, $\mathbf{P} = [P_1, P_2, \dots, P_m]$, and $\boldsymbol{\alpha} = [\alpha_1, \alpha_2, \dots, \alpha_m]$ are the vectors of CRAC supply temperatures, CRAC fan speeds, server powers, and server air flow rates, respectively.

Definition 2 (Output): The output of CFD is a steady-state temperature and air velocity distribution map. For CFD model calibration, we focus on a set of results within the map at the locations installed with temperature sensors, which is denoted by $\hat{\mathbf{T}}_s = [\hat{T}_{s1}, \hat{T}_{s2}, \dots, \hat{T}_{sn}]$.

Definition 3 (Measurement): The measurement is a vector of real temperature values recorded by the physical sensors, which is denoted by $\mathbf{T}_s = [T_{s1}, T_{s2}, \dots, T_{sn}]$.

Let $\|\cdot\|_2$ denotes the ℓ_2 -norm of a vector. With the above definitions, the CFD model calibration aims to find the server

air flow rate configuration that minimizes the ℓ_2 -norm of the error vector between the model output and the measurement:

$$\begin{aligned} \boldsymbol{\alpha}^* &\triangleq \arg \min_{\boldsymbol{\alpha}} \|\tilde{\mathbf{T}}_s(\mathbf{x}) - \mathbf{T}_s\|_2^2, \\ \text{s.t. } \alpha_i^l &\leq \alpha_i \leq \alpha_i^u \text{ for } i = 1, \dots, m. \end{aligned} \quad (1)$$

where $\boldsymbol{\alpha}^*$ is the vector of calibrated air flow rates. Each element in $\boldsymbol{\alpha}^*$ should be within an empirically estimated range $[\alpha^l, \alpha^u]$. In practice, the servers of the same type in general have the same air flow rate. Thus, for a data center with q types of servers, the air flow rate type vector can be reduced as $\boldsymbol{\alpha} = [\alpha_1, \alpha_2, \dots, \alpha_q]$.

C. Approach Overview

Due to the computational cost of solving a high fidelity CFD model, directly solving the optimization problem in Eq. (1) using search algorithms incurs extremely high computation overhead. To address this issue, we design a surrogate model of the CFD model as illustrated in Fig. 1. Let $\hat{\mathbf{T}}_s \in \mathbb{R}^{1 \times n}$ denote the temperature output vector of the surrogate model. Then, the problem in Eq. (1) is converted to a surrogate-based optimization problem that can be solved by iterating two consecutive steps. First, the surrogate model is trained to be locally aligned with the CFD model by minimizing the following objective function:

$$g(\mathbf{w}) \triangleq \|\tilde{\mathbf{T}}_s(\mathbf{x}) - \hat{\mathbf{T}}_s(\mathbf{w}, \mathbf{x})\|_2^2. \quad (2)$$

where \mathbf{w} is a set of trainable weights of the surrogate model. Let \mathbf{w}^* denote the result of the surrogate training. Once \mathbf{w}^* is obtained, the surrogate is then re-optimized such that the discrepancy between the surrogate's output and the measurement is minimized:

$$\boldsymbol{\alpha}^* \triangleq \arg \min_{\boldsymbol{\alpha}} \|\hat{\mathbf{T}}_s(\boldsymbol{\alpha}, \mathbf{w}^*) - \mathbf{T}_s\|_2^2. \quad (3)$$

If the surrogate approaches to the CFD model, the $\boldsymbol{\alpha}^*$ given by Eq. (3) after the convergence of the two-step iterations will approach to the one given by Eq. (1). To address the challenges discussed in §I, we propose to build a knowledge-based GNN surrogate that can capture the physical layout and thermal relations among a number of key variables of a considered data hall. GNN is a machine learning method that models a set of objects using nodes and their relationships using edges on graph domain [28]. For a data hall, we model a set of facilities (i.e., CRACs, servers and sensors) in the considered hall as nodes and their connections as edges into a directed graph. The direction of an edge characterizes the thermal causality between the two end nodes of the edge. For example, an edge points from a CRAC node to a server node, because the supply air temperature of the CRAC affects the inlet temperature of the server. The normalized reciprocal distance between two facilities is used as the initial weight of the edge connecting the corresponding two nodes in the graph. Thus, the initial weight characterizes the intensity of the thermal causality between two facilities. When two facilities are far from each other, the corresponding weight is forced to be zero. This GNN modeling

approach reduces the number of weights and captures the prior knowledge that the temperature measured by a sensor is mostly affected by the facilities in its neighborhood.

IV. CFD CALIBRATION VIA NEURAL SURROGATE

In this section, we present the design of the knowledge-based GNN as a surrogate model that can capture the layout and several key variables of a considered data hall. Then, we present the details of the iterative two-step CFD model calibration using the GNN surrogate.

A. The Architecture of GNN

The GNN aims to capture the complex thermodynamics encompassed in the CFD model. If the GNN can predict the temperatures accurately, it can serve as a surrogate of the CFD model to calibrate the server air flow rates. Moreover, an efficient training of the GNN with a small amount of data generated from CFD is desirable, since the data generation requires intensive computation. The proposed GNN architecture is shown in Fig. 3. It consists of a cooling block and a heating block, which captures the processes of the air flows from the CRACs to the servers and those passing through the servers, respectively. In particular, the input of the model is collected or estimated from a data hall at a time instant, which includes CRAC supply temperatures, CRAC fan speeds, server powers, and server air flow rates. The output is a vector of predicted temperature values corresponding to the sensor measurements.

1) *Cooling block*: For cold aisles, the sensors are installed at the inlet of the servers. In the steady-state, the server inlet temperatures are mainly affected by the CRAC supply temperatures \mathbf{T}_c and fan speeds \mathbf{V} . We initialize the weight of each edge between two nodes representing two facilities with the reciprocal of the physical distance between the two facilities. When the normalized reciprocal is lower than a threshold, the weight is forced to be zero, indicating that the thermal correlation between the two facilities that are far from each other is negligible. Let $\mathbf{W}^{cs} \in \mathbb{R}^{l \times m}$, $\mathbf{W}^{ss} \in \mathbb{R}^{m \times n}$ denote the two matrices consisting of the initialized weights from CRACs to servers and servers to sensors, respectively. Then, the inlet temperature of the j^{th} server that is directly influenced by all CRACs is given by:

$$T_j^{\text{in}} = \sum_{i=1}^l T_i \times p_{ij} \quad \text{for } j = 1, \dots, m. \quad (4)$$

where p_{ij} is a coefficient characterizing the impact of the i^{th} CRAC on the j^{th} server. From intuition, this coefficient is positively related to the CRAC fan speed and the reciprocal distance between the CRAC to the server. In other words, if the CRAC with high fan speed is close to the server, the coefficient is expected to be high and vice versa. Thus, we use the following *softmax* activation function to compute the coefficient p_{ij} :

$$p_{ij} = \frac{e^{z_{ij}}}{\sum_{a=1}^l e^{z_{aj}}}, \quad (5)$$

$$z_{ij} = V_i \times W_{ij}^{cs} \quad \text{for } i = 1, \dots, l. \quad (6)$$

The multiplication in Eq. (6) represents the positive correlation between the temperature coefficient and the two variables, i.e., the CRAC fan speed and the reciprocal distance between the CRAC to the server. With the inlet temperature of servers given by Eq. (4), the temperature at the location of the k^{th} sensor can be predicted by:

$$T_k^{\text{cold}} = \sum_{j=1}^m T_j^{\text{in}} \times W_{jk}^{ss} \quad \text{for } k = 1, \dots, n. \quad (7)$$

2) *Heating block*: The air is heated when it passes through the servers from the cold aisle to the hot aisle. The outlet heat Q^{out} of a server equals the sum of the inlet heat Q^{in} and the server's generated heat Q^{server} . We assume that the energy dissipated from the servers in the forms of electromagnetic radiation and mechanical movements is negligible compared to that dissipated in the form of heat. Thus, Q^{server} is considered to be equal to the server power consumption P . The above energy conversion can be further translated into the temperature domain as [27]:

$$T^{\text{out}} = T^{\text{in}} + \frac{P}{c_p \alpha}. \quad (8)$$

where c_p is a constant representing the specific heat capacity of air, α is the server air flow rate and $\frac{P}{c_p \alpha}$ is the temperature rise. Thus, we represent this knowledge by combining server powers and air flow rates to predict the hot aisle temperature at the location of the k^{th} sensor by:

$$T_k^{\text{hot}} = T_k^{\text{cold}} + \Delta T_k, \quad (9)$$

$$\Delta T_k = a_k X_k + b_k. \quad (10)$$

where ΔT_k is the increased temperature of the k^{th} sensor and can be predicted using a linear scale layer, a_k and b_k are the k^{th} weight and bias, X_k is the input feature of the k^{th} node and can be modeled based on the physical law in Eq. (8) as:

$$X_k = \sum_{j=1}^m \frac{P_j}{\alpha_j} \times W_{jk}^{ss}. \quad (11)$$

where P_j and α_j are the power and air flow rate of the j^{th} server, respectively.

Let $\mathbf{v} \in \{0, 1\}^n$ denote a one-hot vector of sensor types, in which the elements corresponding to the cold aisle sensors are set to 1 and those corresponding to the hot aisle sensors are set to 0. To separate the predicted temperature, the k^{th} output of the GNN surrogate is given by:

$$\hat{T}_{sk} = \begin{cases} T_k^{\text{cold}} \times v_k, & \text{if } v_k = 1, \\ T_k^{\text{hot}} \times (1 - v_k), & \text{if } v_k = 0. \end{cases} \quad (12)$$

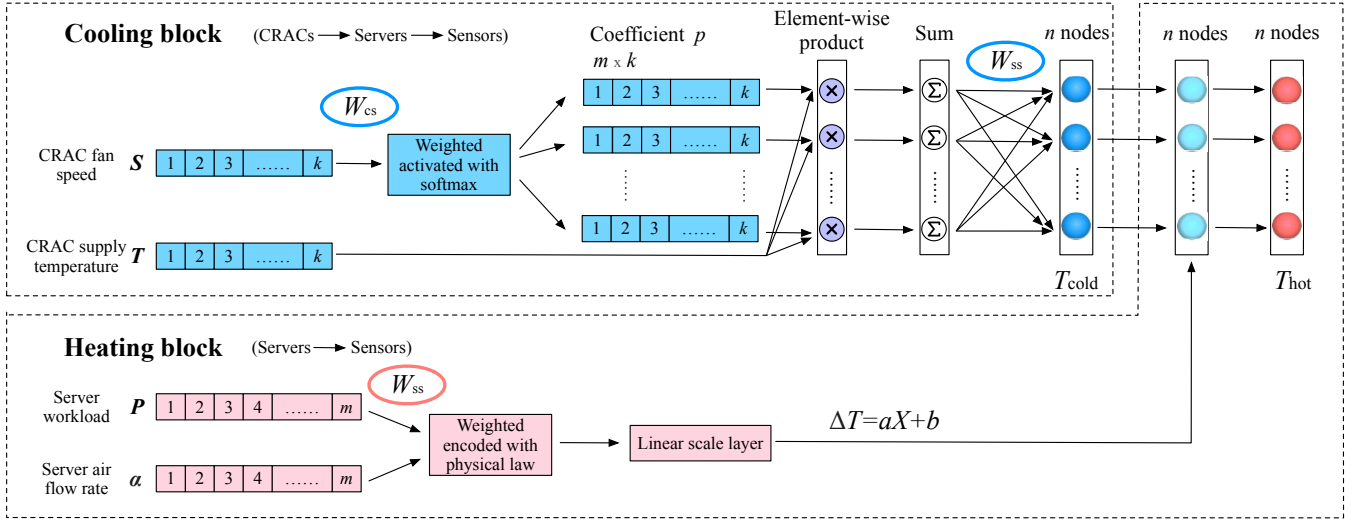


Fig. 3. The architecture of the proposed GNN for temperature prediction. The structure consists of a cooling block and a heating block. A linear scale layer is used to predict the temperature rise induced by servers. The weight between two facilities is initialized using their normalized reciprocal distance.

where v_k is the k^{th} element of \mathbf{v} . With the one-hot vector denoting sensor types, we can represent temperature output for both cooling and heating block in the form of neural net.

In summary, the training phase of the GNN will require the layout of the data hall and the measurements of CRAC supply temperatures, CRAC fan speeds, server powers, and inlet/outlet temperatures. When the trained GNN is used as a surrogate, it can predict the inlet/outlet temperatures given any candidate server air flow rates configuration.

B. Iterative Two-step Optimization

Let \hat{T}_{sk} , \tilde{T}_{sk} , T_{sk} denote the surrogate predicted temperature, the CFD simulated temperature and the measured temperature at the location of the k^{th} sensor, respectively. The optimization is performed by iteratively executing two consecutive steps as overviewed in §III-C. First, the neural surrogate is updated to minimize the errors between its predicted temperatures and the CFD simulated temperatures. Thus, the parameters are updated using the gradient of the weighted least squares loss function, which is given by:

$$\mathcal{L}_1 = \frac{1}{n} \sum_{k=1}^n (\hat{T}_{sk}(\mathbf{W}, \mathbf{x}) - \tilde{T}_{sk}(\mathbf{x}))^2 \times \mu_k. \quad (13)$$

where \mathbf{W} is a set of trainable weights of the surrogate model (i.e., the internal weights of the GNN), and μ_k is an accumulated error of the k^{th} sensor from each calibration iteration. Such error serves as a weight for calculating the loss function, allowing us to focus on the temperatures with high predicted errors.

Once the surrogate is trained to align with the CFD model, the internal weights \mathbf{w} are frozen. The surrogate is then re-optimized to minimize the errors between its predicted temperatures and the measured temperatures by updating the air flow rate configuration of servers. An empirical regularization term is added to penalize the loss function if the temperature

difference between the hot and cold aisle is out of the range $[6^\circ\text{C}, 16^\circ\text{C}]$. The regularization term is expressed using the rectified linear units (ReLU) as:

$$h(T) = \sum_{j=1}^m (\text{ReLU}(6 - \Delta T) + \text{ReLU}(\Delta T - 16)) \times P_j. \quad (14)$$

where P_j is the j^{th} server power. The term means the higher the power is, the more significant the penalty will be. The second loss function with regularization is given by:

$$\mathcal{L}_2 = \frac{1}{n} \sum_{k=1}^n ((\hat{T}_{sk}(\boldsymbol{\alpha}) - T_{sk})^2 \times \nu_k) + \frac{\lambda}{n} \sum_{k=1}^n (h(T) \times \nu_k). \quad (15)$$

where λ is a regularization coefficient, ν_k is similar to μ_k , which is calculated by the errors between the surrogate prediction and the measurement. To accelerate the optimization, we implement a hybrid approach of combining differential evolution algorithm with gradient backpropagation to minimize the loss function \mathcal{L}_2 . Differential evolution is a metaheuristic algorithm for global optimization. The combination of differential evolution and backpropagation has been shown effective in accelerating the training process [29]. The hybrid approach can also reduce the chance that the training process falls into local optimums. The training acceleration by the hybrid approach will also be evaluated in §V-B2.

Through iterative optimization of the two loss functions, the air flow rate configuration can be calibrated to increase the accuracy of CFD model with respect to real sensor measurements. Based on the above descriptions, the proposed algorithm for implementing the auto-calibration of CFD model can be summarized in Algorithm 1.

C. Discussion

We now discuss several issues in the implementation of the surrogate-based calibration approach.

Algorithm 1: Surrogate-based Calibration of Data Center CFD Model

Input: Measurements collected from the considered data hall at a time instant, which include CRAC supply temperatures T_c , CRAC fan speeds V , server powers P , and sensor measurements T_s . Initial rough estimations of server air flow rates α .

Result: Calibrated server air flow rates α^*

- 1 Initialize connection weights W^{cs} , W^{ss} using the normalized reciprocals of the distances between facilities, and network weights W randomly.
 - 2 Assign initial settings to the computational graph \mathcal{G} .
 - 3 **for** $i = 1$ **to** max iteration **do**
 - 4 Input $x = [T_c, V, P, \alpha^*]$ to the CFD model.
 - 5 Run one time CFD simulation.
 - 6 Obtain CFD simulation result \tilde{T}_s .
 - 7 Compute surrogate temperature prediction \hat{T}_s .
 - 8 Generate loss weights μ and ν of each sensor.
 - 9 Compute surrogate loss function \mathcal{L}_1 .
 - 10 Perform gradient descent to minimize \mathcal{L}_1 .
 - 11 Compute surrogate loss function \mathcal{L}_2 .
 - 12 Perform differential evolution to search α that minimizes \mathcal{L}_2 .
 - 13 Perform gradient descent on α to minimize \mathcal{L}_2 .
 - 14 **end**
-

Issue 1: The GNN is trained for the purpose of updating the CFD model configuration (i.e., the server air flow rates) at a time instant. Thus, it is not advisable to use the GNN for run-time temperature prediction. The calibrated CFD shall be used for the run-time temperature prediction in improving energy efficiency and reducing operational risks.

Issue 2: The proposed GNN is designed for data halls with hot aisle containments. Thus, heat recirculation is not considered in the above architecture. To extend the GNN to address the data halls without containments, heat recirculation and temperature mixing effects can be added to the GNN.

Issue 3: In this paper, we mainly focus on temperature calibration of CFD models. For other configuration parameters that have a similar calibration problem, the proposed approach can be extended to address them with proper surrogate design. With installed air flow rate sensor, the proposed approach can also be further extended to address the air velocity distributions of CFD models.

V. PERFORMANCE EVALUATION

In this section, we apply our surrogate-based approach to calibrate the CFD models built for two production data halls and present the evaluation results.

A. Testbed and Dataset

We build two CFD models based on a commercial software [30] for two production data halls (referred to as Hall A and B) sized hundreds of square meters that host thousands of

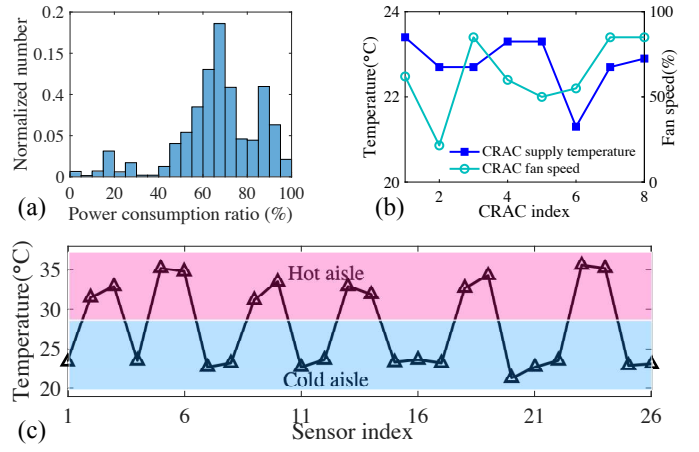


Fig. 4. Data collected from Hall B at a time instant. (a) Server power distributions; (b) CRAC supply temperatures and fan speeds; (c) sensor measurements

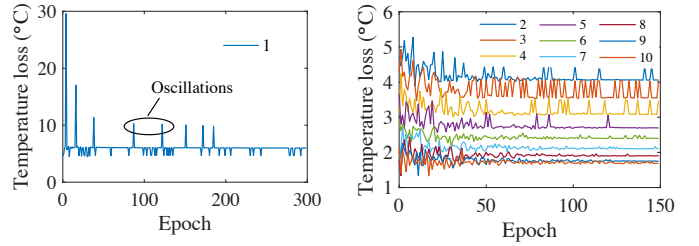


Fig. 5. Temperature training loss in 10 iterations of calibration iteration. (a) 1st iteration; (b) subsequent iterations. With adaptively decreased learning rate and newly appended training data, the loss curve gradually becomes stable and convergent.

servers¹, respectively. These two halls mainly provide service for e-commerce sales.

Fig. 4 shows an example of data collected from Hall B at a time instant. Fig. 4 (a) is the distribution of the normalized server powers. We can see that most servers are working at approximately 60% of its maximum power. However, the distribution is not uniform given different server types and workload status. The cold aisle sensor measurements range from 20°C to 24°C, which is close to the CRAC supply temperatures. The hot aisle sensor measurements range from 30°C to 36°C at different locations, which are affected by the generated heat from the servers.

B. Approach Evaluation

To implement our proposed approach, we implement the proposed GNN architecture as a computational graph using Google Tensorflow [31]. We choose Adam [32] as the optimizer, which is a method for efficient stochastic optimization that only requires first-order gradients with little memory requirement. Given the limited training data generated from the CFD model, we start the training process of the GNN with only three samples at a time instant. The three samples

¹The specific configurations are confidential due to commercial interest.

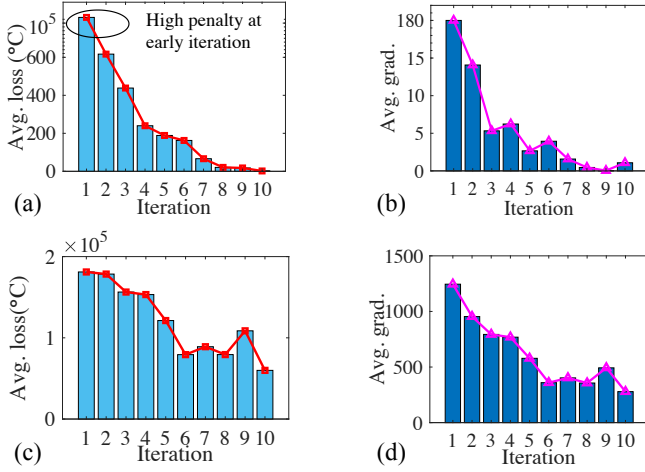


Fig. 6. Average loss and gradient for each calibration iteration when updating α using different approaches. (a) Loss with differential evolution; (b) gradient with differential evolution; (c) loss without differential evolution; (d) gradient without differential evolution.

are generated by configuring the server air flow rates with their lower and upper bounds, as well as a mid point between the bounds. Each sample consists of the temperatures computed by the CFD model at the sensor locations. To prevent over-fitting, we also add Gaussian noise to the training data to augment the training batch size. Such an approach follows the study in [33], which is shown effective for improving the training process. The augmented batch size for each sample is $B = 10$. Thus, we have a total of 30 samples for the initial training process. New data is appended for re-training after each calibrated iteration with updated air flow rate configuration and the corresponding CFD simulation results. Besides, the training epoch is first set to $E = 300$ for the first iteration, and then reduced to $E = 150$ for subsequent iterations. The learning rate for updating \mathbf{W} is initialized to $\eta_1 = 0.1$ for fast learning and then adaptively decreased with a coefficient 0.8 for subsequent iterations. The learning rate for updating α is set to $\eta_2 = 0.001$. The regularization coefficient is set to $\lambda = 1$. The maximum calibration iteration is set to $i = 10$.

1) *Surrogate Training*: Fig. 5 shows the training loss of the GNN surrogate in 10 iterations of calibration. For the initial training, the curve fluctuates due to the large learning rate and limited training data. After iterations of surrogate training with decreased learning rate and newly appended data, the loss curves gradually become stable and convergent.

2) *Flow Rate Updating*: To evaluate the flow rate updating with different approaches, we calculate the average loss and gradient variation of all epochs for each iteration. Fig. 6 (a) and (b) show the average loss and the gradient of each calibration iteration when performing Adam optimization on α after differential evolution. For the first iteration, the loss and gradient are quite large, indicating the regularization penalty in Eq. (15) is significant at the early iterations. For subsequent iterations, the average loss gradually decreases to zero. Meanwhile, the average gradient also gets close to zero

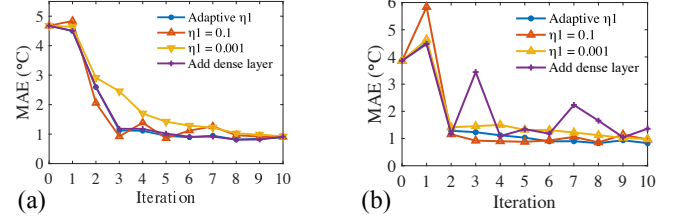


Fig. 7. CFD predicted temperature MAE at sensor locations for each iteration with different learning rate and net architecture. (a) Hall A; (b) Hall B.

with increasing iterations. Fig. 6 (c) and (d) show the average loss and gradient of directly updating α without using the differential evolution search before. It can be seen that the updating speed is quite slow, and the average loss is still large after 10 iterations. Therefore, the differential evolution can help accelerate the convergence speed by constraining the gradient updating in a specific region.

3) *Calibration Results*: In this section, we evaluate the calibrated results of the CFD models using our proposed approach. To perform the test, the CFD solver is running in parallel on 4 processor cores. Each test is solved with 1,000 iterations in the steady-state mode. To evaluate the performance, we use the metric *mean absolute error* (MAE), which is defined by $MAE = \frac{1}{N} \sum_{i=1}^N |y_i - \hat{y}_i|$ where N is the number of samples, y_i and \hat{y}_i are the ground truth and calibrated results, respectively. Fig. 7 shows the MAE variation in 10 iterations with different learning rate η_1 . With adaptive setting of η_1 , the MAE of the simulated and real temperatures of the two halls achieves the lowest value of 0.81°C and 0.75°C , respectively. We also add two densely connected layers in the cooling block to increase the complexity of the GNN architecture. However, with increased complexity, the performance does not improve much. A potential reason is that the training data is limited. Increasing the net complexity may not help improve the performance of the GNN surrogate.

Fig. 8 (a) and Fig. 9 (a) show the thermal result planes of the two halls that are solved in uncalibrated CFD models. It can be seen that the temperature distribution is uneven for both cold and hot aisles. Such results diverge significantly from the ground truth due to inaccurate estimation of the server air flow rates, which could have a great influence on thermal distribution in the inlet and outlet of servers. Fig. 8 (b) and Fig. 9 (b) show the best-calibrated result planes based on our proposed algorithm within 10 iterations. After calibration, the temperature distribution becomes more uniform. To numerically compare the results, we take the sensor measurements as the ground truth for analysis. Fig. 8 (c) and Fig. 9 (c) show the temperature values at the sensor locations of the calibrated models versus the uncalibrated models of the two halls. From the results, an uncalibrated CFD model can generate temperature prediction errors from 3°C to 6°C . After calibration, the simulated temperatures can well match the sensor measurements at corresponding locations and the MAEs are 0.81°C and 0.75° , respectively. The results

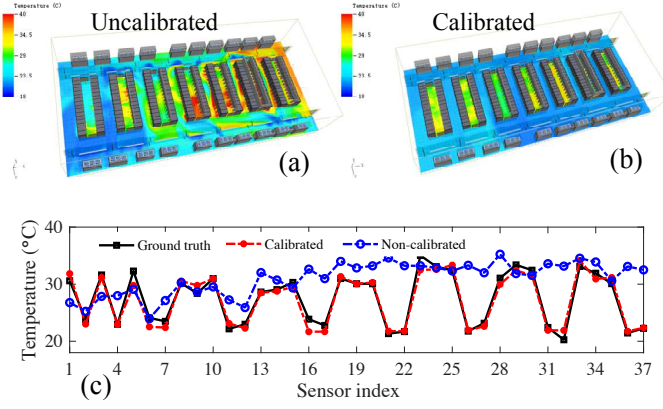


Fig. 8. Steady-state temperature distribution of Hall A. (a) Uncalibrated thermal planes; (b) calibrated thermal planes; (c) temperature values at sensor locations.

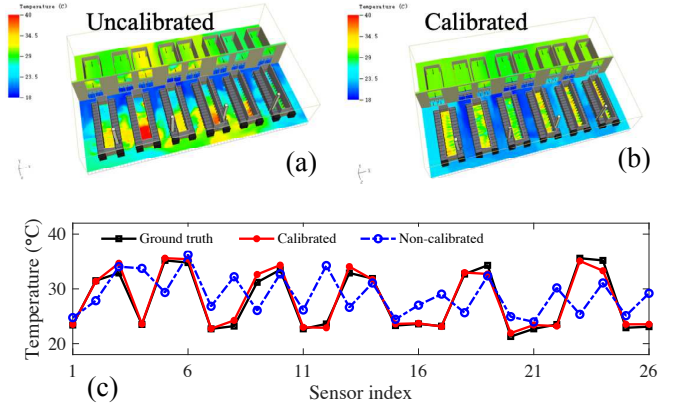


Fig. 9. Steady-state temperature distribution of Hall B. (a) Uncalibrated thermal planes; (b) calibrated thermal planes; (c) temperature values at sensor locations.

indicate the calibrated model has high fidelity and can be representative for production data centers.

C. Comparisons with Baseline Approaches

The proposed surrogate-based approach for automated calibration is then compared with other three baselines under identical settings. The baselines are listed as follows:

- *Manual Calibration*: The manual calibration process is achieved by extensively flow rate tuning in the CFD model with assistance from a domain expert with years of experience in CFD modeling. Specifically, if the simulated temperature is higher than the real temperature measurement, the expert empirically increases the flow rate of nearby servers and vice versa.
- *Vanilla Neural Surrogate*: A vanilla neural net is used as the surrogate model for the CFD calibration. Unlike the proposed knowledge-based GNN architecture, the vanilla neural net does not capture the information dependency between nodes. Instead, it forwards information with densely connected edges and randomly initializes Gaussian weights to the edges.
- *CMA-ES*: This baseline stands for covariance matrix adaptation evolution strategy, which is a derivative-free optimization method for numerical optimization. Here, we use the (1+1) strategy proposed in [34] to generate only one candidate solution per iteration. If the MAE of the new offspring is better, it becomes the parent. The mutation rate is set to $\sigma = 5$ and adaptively adjusted for each iteration.

Fig. 10 shows the MAE comparison for temperature prediction after calibration with different approaches. From the figures, we can see that our proposed method achieves lower MAEs compared to other baselines on both halls. Since the training data is limited, the vanilla neural surrogate cannot be trained to well represent the complex CFD model. Similarly, with only 10 iterations, the CMA-ES approach that employs heuristic search cannot obtain the optimal flow rate configuration. Although the manual calibration with the help of a

domain expert can reduce the MAE to about 1.1°C , it is quite labor-intensive. Therefore, our proposed approach is effective for automated calibration of CFD models built for large-scale data halls.

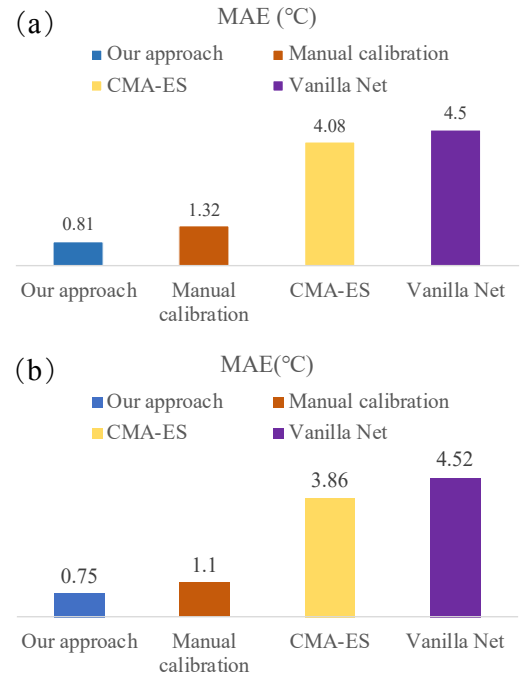


Fig. 10. Comparison of MAE of different calibration approaches. (a) Hall A, (b) Hall B.

D. Effectiveness of Calibrated Model over Time

In this section, we evaluate our approach over long-term test in Hall A. Specifically, the calibrated server air flow rate configuration at a time instant are saved into a library and then imported for test using data collected within one month (01 Nov. to 30 Nov. , 2018). Fig. 11 shows a pair of cold and hot aisle sensor measurements and the corresponding CFD

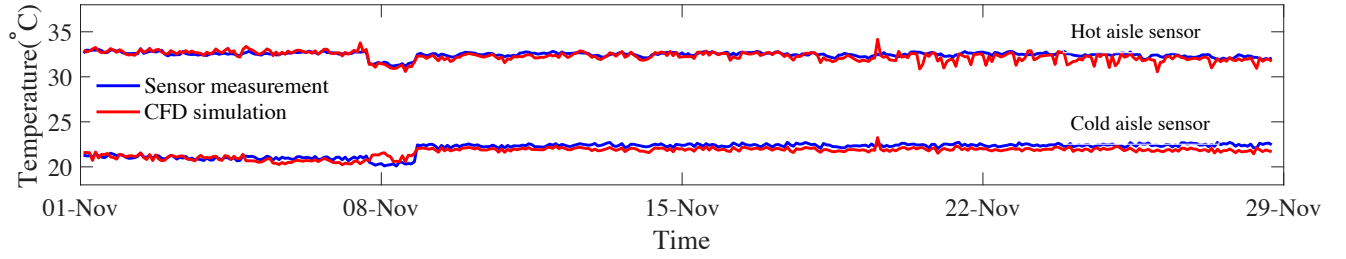


Fig. 11. Temperature evaluation over one month. Red line: CFD simulated temperatures with calibrated air flow rate configuration at sensor locations. Blue line: real measurements of corresponding cold and hot aisle sensors.

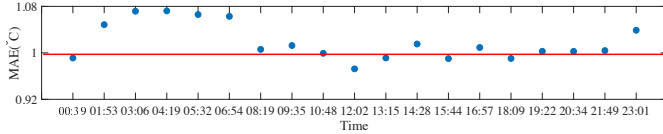


Fig. 12. Temperature prediction MAE during an online peak day for shopping carnival

predicted temperatures over this period. The sampling period for the test is one hour. From the figure, we can observe that the predicted results well match the measurements for both cold and hot aisle sensors. The hot aisle sensor exhibits slightly larger prediction errors. This is due to the hot aisle suffers more influence from server powers and hence have more complex thermal behaviors.

Next, we consider servers with high workload, which is different from the workload status used for the calibration. Given the tested data halls mainly provide service for e-commerce sales, we take an online shopping carnival day for analysis. Fig. 12 shows the MAE of temperature prediction on this day based on the calibrated model. From the figure, we can see that the temperature MAE varies around 1°C. The increased error indicates when the servers work on a peak status, the thermal behaviors will be more complex in the data hall, rendering the decreased accuracy of CFD model prediction.

E. Computation Overhead

To evaluate the time needed for the CFD model calibration, we perform test with different CPU cores. As discussed in §I, the calibration aims to find the optimal air flow rate configuration while requires the fewest CFD model forwarding processes. Based on above evaluations, our proposed surrogate-based calibration achieves lower error within 10 iterations. In other word, the temperature prediction MAE of both halls can decrease to 0.81°C and 0.75°C within only 10 times CFD forwarding processes. With more iterations, we found the MAE can be further reduced to 0.76°C and 0.59°C after 15 times of calibration iteration.

Fig. 13 shows the running time required for solving the CFD model with different CPU cores. In our test with 4 CPU cores, the required time for 10 times CFD forwarding is 25.4 hours. The average time for each iteration of surrogate training is 0.5

hours. Thus, with above basic settings, the calibration can be finished in around 30 hours.

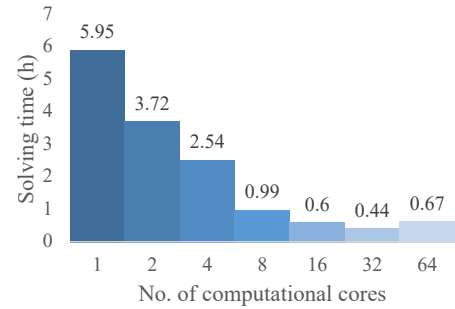


Fig. 13. CFD solved with different number of cores in 1,000 iterations with 10 million grid cells and 11,982 objects.

VI. CONCLUSION

This paper proposes an automated surrogate-based approach to calibrate CFD models of data centers. We adopt a knowledge-based GNN to build the surrogate model. The proposed approach can capture the thermal relations among a number of key variables in the physical infrastructures and reduce the demand on the amount of training data. For two CFD models built for two production data halls that host thousands of servers, our approach achieves temperature prediction MAEs of 0.81°C and 0.75°C. In contrast, the heuristic calibration and manual calibration achieve about MAEs of 4°C and more than 1°C, respectively. The improvement of up to 0.5°C is significant in CFD modeling due to the sharply increased difficulty in improving accuracy when the errors are already low (i.e., at around 1°C). Thus, our automated neural surrogate calibration approach is promising for promoting the existing CFD models constructed for data centers to their digital twin forms. Our approach also sheds lights on the calibration of compute-intensive models to pursue high accuracy in approximating complex physical processes.

ACKNOWLEDGMENT

This work is funded by National Research Foundation (NRF) via the Green Data Centre Research (GDCR) and the Green Buildings Innovation Cluster (GBIC), administered by

REFERENCES

- [1] Cisco global cloud index: Forecast and methodology, 2016/2021 white paper. [Online]. Available: <http://www.cisco.com/c/en/us/solutions/collateral/service-provider/>
- [2] M. Wiboonrat, "Data center infrastructure management WLAN networks for monitoring and controlling systems," in *The International Conference on Information Networking 2014 (ICOIN)*, 2014, pp. 226–231.
- [3] M. Shafto, M. Conroy, R. Doyle, E. Glaessgen, C. Kemp, J. LeMoigne, and L. Wang, "Draft modeling, simulation, information technology & processing roadmap," *Technol. Area*, vol. 11, 2010.
- [4] B. Bielefeldt, J. Hochhalter, and D. Hartl, "Computationally efficient analysis of SMA sensory particles embedded in complex aerostructures using a substructure approach," in *ASME 2015 Conference on Smart Materials, Adaptive Structures and Intelligent Systems*, 2015.
- [5] E. J. Tuegel, A. R. Ingraffea, T. G. Eason, and S. M. Spottswood, "Reengineering aircraft structural life prediction using a digital twin," *Int. J. Aerosp. Eng.*, vol. 2011, 2011.
- [6] B. Smarslok, A. Culler, and S. Mahadevan, "Error quantification and confidence assessment of aerothermal model predictions for hypersonic aircraft," in *53rd AIAA/ASME/ASCE/AHS/ASC Structures, Structural Dynamics and Materials Conference 20th AIAA/ASME/AHS Adaptive Structures Conference 14th AIAA*, 2012, p. 1817.
- [7] Q. Qi and F. Tao, "Digital twin and big data towards smart manufacturing and industry 4.0: 360 degree comparison," *IEEE Access*, vol. 6, pp. 3585–3593, 2018.
- [8] K. M. Alam and A. El Saddik, "C2PS: A digital twin architecture reference model for the cloud-based cyber-physical systems," *IEEE Access*, vol. 5, pp. 2050–2062, 2017.
- [9] N. Mohammadi and J. E. Taylor, "Smart city digital twins," in *2017 IEEE Symposium Series on Computational Intelligence (SSCI)*, 2017, pp. 1–5.
- [10] A. Radmehr, B. Noll, J. Fitzpatrick, and K. Karki, "CFD modeling of an existing raised-floor data center," in *29th IEEE Semiconductor Thermal Measurement and Management Symposium*, 2013, pp. 39–44.
- [11] Y. Ran, H. Hu, X. Zhou, and Y. Wen, "DeepEE: Joint optimization of job scheduling and cooling control for data center energy efficiency using deep reinforcement learning," in *2019 IEEE 39th International Conference on Distributed Computing Systems (ICDCS)*, 2019, pp. 645–655.
- [12] P. M. Watson and K. C. Gupta, "Design and optimization of CPW circuits using EM-ANN models for CPW components," *IEEE Trans. Microw. Theory Tech.*, vol. 45, no. 12, pp. 2515–2523, 1997.
- [13] U. Singh, A. Singh, S. Parvez, and A. Sivasubramaniam, "CFD-based operational thermal efficiency improvement of a production data center," in *SustainIT*, 2010.
- [14] J. Mockus, *Bayesian approach to global optimization: Theory and applications*. Springer Science & Business Media, 2012, vol. 37.
- [15] J. H. Holland, "Genetic algorithms," *Sci.Am.*, vol. 267, no. 1, pp. 66–73, 1992.
- [16] J. Moore, J. S. Chase, and P. Ranganathan, "Weatherman: Automated, online and predictive thermal mapping and management for data centers," in *2006 IEEE international conference on Autonomic Computing*, 2006, pp. 155–164.
- [17] D. Yi, X. Zhou, Y. Wen, and R. Tan, "Toward efficient compute-intensive job allocation for green data centers: A deep reinforcement learning approach," in *2019 IEEE 39th International Conference on Distributed Computing Systems (ICDCS)*, 2019, pp. 634–644.
- [18] L. Li, C.-J. M. Liang, J. Liu, S. Nath, A. Terzis, and C. Faloutsos, "Thermocast: A cyber-physical forecasting model for datacenters," in *Proceedings of the 17th ACM SIGKDD International Conference on Knowledge Discovery and Data Mining*, 2011, pp. 1370–1378.
- [19] J. Chen, R. Tan, Y. Wang, G. Xing, X. Wang, X. Wang, B. Punch, and D. Colbry, "A high-fidelity temperature distribution forecasting system for data centers," in *2012 IEEE 33rd Real-Time Systems Symposium*, 2012, pp. 215–224.
- [20] S. Koziel and L. Leifsson, "Surrogate-based aerodynamic shape optimization by variable-resolution models," *AIAA J.*, vol. 51, no. 1, pp. 94–106, 2012.
- [21] J. W. Bandler, R. M. Biernacki, S. H. Chen, P. A. Grobelny, and R. H. Hemmers, "Space mapping technique for electromagnetic optimization," *IEEE Trans. Microw. Theory Tech.*, vol. 42, no. 12, pp. 2536–2544, 1994.
- [22] W. Na, F. Feng, C. Zhang, and Q.-J. Zhang, "A unified automated parametric modeling algorithm using knowledge-based neural network and l_1 optimization," *IEEE Trans. Microw. Theory Tech.*, vol. 65, no. 3, pp. 729–745, 2016.
- [23] M. J. Asher, B. F. Croke, A. J. Jakeman, and L. J. Peeters, "A review of surrogate models and their application to groundwater modeling," *Water Resour. Res.*, vol. 51, no. 8, pp. 5957–5973, 2015.
- [24] Z. Han, C. Xu, L. Zhang, Y. Zhang, K. Zhang, and W. Song, "Efficient aerodynamic shape optimization using variable-fidelity surrogate models and multilevel computational grids," *Chin. J. Aeronaut.*, 2019.
- [25] J. W. Bandler, R. M. Biernacki, S. H. Chen, R. H. Hemmers, and K. Madsen, "Electromagnetic optimization exploiting aggressive space mapping," *IEEE Trans. Microw. Theory Tech.*, vol. 43, no. 12, pp. 2874–2882, 1995.
- [26] P. J. Roache, *Computational fluid dynamics*. Hermosa publishers, 1972, no. BOOK.
- [27] M. Jonas, R. R. Gilbert, J. Ferguson, G. Varsamopoulos, and S. K. S. Gupta, "A transient model for data center thermal prediction," in *2012 International Green Computing Conference (IGCC)*, 2012, pp. 1–10.
- [28] J. Zhou, G. Cui, Z. Zhang, C. Yang, Z. Liu, L. Wang, C. Li, and M. Sun, "Graph neural networks: A review of methods and applications," *arXiv preprint arXiv:1812.08434*, 2018.
- [29] L. Wang, Y. Zeng, and T. Chen, "Back propagation neural network with adaptive differential evolution algorithm for time series forecasting," *Expert Syst. Appl.*, vol. 42, no. 2, pp. 855–863, 2015.
- [30] "6sigmadcx." [Online]. Available: <https://www.futurefacilities.com>
- [31] M. Abadi, P. Barham, J. Chen, Z. Chen, A. Davis, J. Dean, M. Devin, S. Ghemawat, G. Irving, M. Isard *et al.*, "Tensorflow: A system for large-scale machine learning," in *12th USENIX Symposium on Operating Systems Design and Implementation (OSDI 16)*, 2016, pp. 265–283.
- [32] D. P. Kingma and J. Ba, "Adam: A method for stochastic optimization," *arXiv preprint arXiv:1412.6980*, 2014.
- [33] C. M. Bishop, "Training with noise is equivalent to tikhonov regularization," *Neural Comput.*, vol. 7, no. 1, pp. 108–116, 1995.
- [34] C. Igel, T. Suttorp, and N. Hansen, "A computational efficient covariance matrix update and a (1+1)-CMA for evolution strategies," in *Proceedings of the 8th annual conference on Genetic and evolutionary computation*, 2006, pp. 453–460.